Regular Article

MYELOID NEOPLASIA

miR-155 promotes FLT3-ITD–induced myeloproliferative disease through inhibition of the interferon response

Jared A. Wallace,[1] Dominique A. Kagele,[1] Anna M. Eiring,[2] Carissa N. Kim,[1] Ruozhen Hu,[1] Marah C. Runtsch,[1] Margaret Alexander,[1] Thomas B. Huffaker,[1] Soh-Hyun Lee,[1] Ami B. Patel,[2] Timothy L. Mosbruger,[2] Warren P. Voth,[1] Dinesh S. Rao,[3] Rodney R. Miles,[1,2] June L. Round,[1] Michael W. Deininger,[2,4] and Ryan M. O'Connell[1]

[1]Department of Pathology and [2]Huntsman Cancer Institute, University of Utah, Salt Lake City, UT; [3]Department of Pathology, University of California Los Angeles, Los Angeles, CA; and [4]Division of Hematology and Hematologic Malignancies, Huntsman Cancer Institute, University of Utah, Salt Lake City, UT

Key Points

- miR-155 promotes myeloproliferation in the bone marrow, spleen, and blood of mice carrying the FLT3-ITD mutation.
- miR-155 suppresses the IFN response in FLT3-ITD⁺ mouse hematopoietic stem and progenitor cells, as well as FLT3-ITD⁺ human AML cells.

FLT3-ITD⁺ acute myeloid leukemia (AML) accounts for ~25% of all AML cases and is a subtype that carries a poor prognosis. microRNA-155 (miR-155) is specifically overexpressed in FLT3-ITD⁺ AML compared with FLT3 wild-type (FLT3-WT) AML and is critical for the growth of FLT3-ITD⁺ AML cells in vitro. However, miR-155's role in regulating FLT3-ITD–mediated disease in vivo remains unclear. In this study, we used a genetic mouse model to determine whether miR-155 influences the development of FLT3-ITD–induced myeloproliferative disease. Results indicate that miR-155 promotes FLT3-ITD–induced myeloid expansion in the bone marrow, spleen, and peripheral blood. Mechanistically, miR-155 increases proliferation of the hematopoietic stem and progenitor cell compartments by reducing the growth-inhibitory effects of the interferon (IFN) response, and this involves targeting of Cebpb. Consistent with our observations in mice, primary FLT3-ITD⁺ AML clinical samples have significantly higher miR-155 levels and a lower IFN response compared with FLT3-WT AML samples. Further, inhibition of miR-155 in FLT3-ITD⁺ AML cell lines using CRISPR/Cas9, or primary FLT3-ITD⁺ AML samples using locked nucleic acid antisense inhibitors, results in an elevated IFN response and reduces colony formation. Altogether, our data reveal that miR-155 collaborates with FLT3-ITD to promote myeloid cell expansion in vivo and that this involves a multitarget mechanism that includes repression of IFN signaling. (*Blood*. 2017;129(23):3074-3086)

Introduction

Acute myeloid leukemia (AML) is an aggressive hematological malignancy that carries a poor prognosis. AML is a heterogeneous disease with a variety of genetic aberrations, including translocations and mutations, that can drive leukemic phenotypes. The most common genetic aberration in AML is a gain-of-function mutation in the FMS-like tyrosine kinase 3 (FLT3) receptor. FLT3 internal tandem duplication (ITD) in the juxtamembrane domain of the receptor occurs in ~25% of AML diagnoses and confers a poor prognosis.[1] FLT3 is a cell surface protein that promotes the proliferation and survival of the hematopoietic stem and progenitor cell (HSPC) compartments in response to FLT3 ligand.[2] However, FLT3-ITD mutations lead to constitutive, ligand-independent activation of this receptor,[3] conferring a growth and survival advantage.

Although FLT3-ITD is a common mutation observed in human AML and carries a poor prognosis, the mutation itself has not been shown to independently drive leukemic transformation in vivo. Rather, FLT3-ITD must collaborate with additional oncogenic mutations to trigger hematopoietic malignancy.[4-6] Introduction of human FLT3-ITD mutations into mice triggers a myeloproliferative disease (MPD) that

resembles chronic myelomonocytic leukemia,[7-9] but does not lead to overt leukemia. Regardless, FLT3-ITD mouse models have proven useful in studying FLT3-ITD biology in hematologic malignancies.

MicroRNAs (miRNAs) are small noncoding RNAs that repress their target genes by binding to cognate sites in the 3′ untranslated region of their respective messenger RNA targets, thereby preventing their translation and/or triggering messenger RNA degradation. miRNA expression has been shown to be highly dysregulated in AML, including FLT3-ITD⁺ AML, where microRNA-155 (miR-155) represents the most significantly overexpressed miRNA.[10-16] Overexpression of miR-155 alone in the hematopoietic compartment is sufficient to cause a myeloproliferative phenotype[17] resembling that seen in mice harboring FLT3-ITD mutations. Although the association between FLT3-ITD and miR-155 overexpression has been observed in primary human samples, and miR-155 has been shown to promote FLT3-ITD⁺ cell line growth in vitro,[18,19] the relationship between FLT3-ITD and miR-155 has not been directly examined in vivo, and the downstream effects of miR-155 overexpression are still being deciphered.

The online version of this article contains a data supplement.

In this study, we used a FLT3-ITD genetic mouse model and FLT3-ITD[+] human AML cells to study the collaboration between the FLT3-ITD mutation and miR-155 in promoting hematologic malignancy. We found that miR-155 substantially contributes to FLT3-ITD–induced MPD, and that knockdown of miR-155 in primary FLT3-ITD[+] AML samples reduces colony formation. Mechanistically, we show that miR-155 inhibits the response to interferon (IFN) in these model systems, and this involves direct repression of Cebpb. Interferon has previously been shown to exhibit an antiproliferative effect on early hematopoietic cells,[20-23] including in our FLT3-ITD mouse model.[24] Altogether, our study identifies a specific role for miR-155 in promoting the expansion of myeloid cells in FLT3-ITD–mediated disease in vivo, indicating that inhibition of miR-155 may be a promising new therapeutic approach for treatment of FLT3-ITD[+] AML.

Methods

A more extensive description of the methods can be found in the supplemental Methods, available on the *Blood* Web site.

Animals

All mice (wild-type [WT], 155[−/−], FLT3-ITD, and FLT3-ITD 155[−/−]) were on a C57BL/6 background. FLT3-ITD mice were obtained from The Jackson Laboratory (stock no. 011112) and were homozygous for the FLT3-ITD mutation. Experimental procedures were performed with the approval of the Institutional Animal Care and Use Committee of the University of Utah.

Flow cytometric analysis

Splenocytes and bone marrow (BM) cells were harvested from mice and depleted of red blood cells prior to staining with specific fluorophore-conjugated antibodies. Antibody-stained cells were analyzed with a BD LSR Fortessa flow cytometer (BD Biosciences), and data analysis was performed by using FlowJo software.

Proliferation assay

FLT3-ITD and FLT3-ITD 155[−/−] mice were injected intraperitoneally with 150 μL of 5-bromo-2′-deoxyuridine (BrdU [BD Pharmingen]) at a concentration of 10 mg/mL 20 hours prior to BM harvest. BM cells were fixed and stained with an anti-BrdU antibody (BD Pharmingen) following the manufacturer's instructions and analyzed via flow cytometry.

BM chimera reconstitutions

Total BM was harvested from FLT3-ITD and FLT3-ITD 155[−/−] mice (45.2[+]) and mixed in equal ratios with BM from WT (45.1[+]) mice purchased from The Jackson Laboratory (stock no. 002014). Myeloproliferative phenotypes were evaluated at 3 months.

Expression profiling

Lineage-negative (Lin[−]), c-Kit[+], Sca1^{+} (LKS) cells were sorted by using flow cytometry, and total RNA was isolated using the miRNeasy spin column kit (Qiagen). RiboZero treatment/library preparation was performed at the University of Utah DNA Sequencing Core Facility, followed by stranded RNA sequencing by using Illumina HiSequation 2000 sequencing. Aligned reads (miRBase) were used in DESeq2 (version 1.10.1), which normalizes the signal and determines differential expression. The RNA sequencing data has been deposited in the National Center for Biotechnology Information Gene Expression Omnibus under GSE86526. Genes with multiple testing corrected *P* values < .05 were used in Ingenuity Pathway Analysis and Gene Set Enrichment Analysis (GSEA). Western blotting and quantitative reverse transcription polymerase chain reaction (qRT-PCR) were carried out by using standard procedures.

Cell culture and lentiCRISPR infections

Molm14 and MV4-11 cell lines were cultured in RPMI 1640 with fetal bovine serum and antibiotics. LentiCRISPR infections (155-CR1 and empty vector [EV]) were performed as described previously,[19] and cells were passaged for at least 10 days prior to analysis.

TCGA analysis

Mirbase20 miRNA expression data from IlluminaGA_miRNASeq (n = 188) and the RSEM gene expression data from IlluminaGA_RNASeqV2 (n = 173) were downloaded from The Cancer Genome Atlas (TCGA) Web site for the available AML samples. Somatic variants for the 305 mutated genes identified in the 200 TCGA AML patients were downloaded from the cBioPortal Web site (http://www.cbioportal.org/). AML samples were split into FLT3-ITD–positive samples (FLT3-ITD) and FLT3 mutation–negative samples (FLT3-WT). DESeq2 (version 1.10.1) was used to normalize the count data and detect differently expressed genes or miRNAs.

Cebpb overexpression

Lin[−] c-Kit[+] (LK) cells were sorted by flow cytometry and cultured in RPMI 1640–based medium with 50 ng/mL SCF. Cells infected with either an EV control (pMIG II-EV) or Cebpb-overexpressing vector (pMIG II-Cebpb) were passaged for 2 days in individual wells prior to RNA isolation.

Patient samples

Mononuclear cells from the peripheral blood of FLT3-ITD^{+} AML patients at the Huntsman Cancer Institute (University of Utah) were Ficoll-separated and used for automated isolation of the CD34^{+} fraction by using an autoMACS Pro (Miltenyi Biotech). Cells were used for methylcellulose colony assays or expanded in liquid culture to assess Annexin V or gene expression by qRT-PCR. Cells were treated with 100 nM LNA-155 or LNA-CTRL (Exiqon). Donors gave informed consent and studies were approved by the University of Utah Institutional Review Board (no. 00045880).

Statistics

Significant *P* values were determined by using an unpaired Student *t* test unless otherwise noted. Quantitative data are displayed as mean ± standard error of the mean (SEM). *P* values are shown as indicated: *$P \leq .05$; **$P \leq .01$; ***$P \leq .001$; ****$P \leq .0001$; and not significant (ns) $P > .05$. The false discovery rate for GSEA plots was calculated by using Limma. All other statistics were performed in either GraphPad Prism 6.0 or Microsoft Excel.

Results

miR-155 promotes expansion of myeloid cells in the spleen and the blood of FLT3-ITD[+] mice

We generated mice homozygous for the FLT3-ITD mutation (denoted as FLT3-ITD) that also lack miR-155 (155[−/−]) to test the function of miR-155 during FLT3-ITD–mediated pathogenesis in vivo (Figure 1A-B). Of note, mice homozygous for the FLT3-ITD mutation develop a chronic MPD during adulthood.[7-9] At 4 to 6 months of age, FLT3-ITD miR-155^{+/+} (FLT3-ITD), FLT3-ITD 155[−/−], WT, and 155[−/−] mice were analyzed. We observed that FLT3-ITD–induced splenomegaly was significantly reduced in the absence of miR-155 (Figure 1C), both in terms of overall spleen weight and cellularity (Figure 1D). Spleens from FLT3-ITD animals showed extensive infiltration of maturing myeloid cells disrupting and replacing the white pulp and had a significant reduction in the red pulp as well as normal erythropoiesis (Figure 1E). Although various aspects of this disease process were still observed in the FLT3-ITD 155[−/−] group, their severity was noticeably diminished compared with their FLT3-ITD
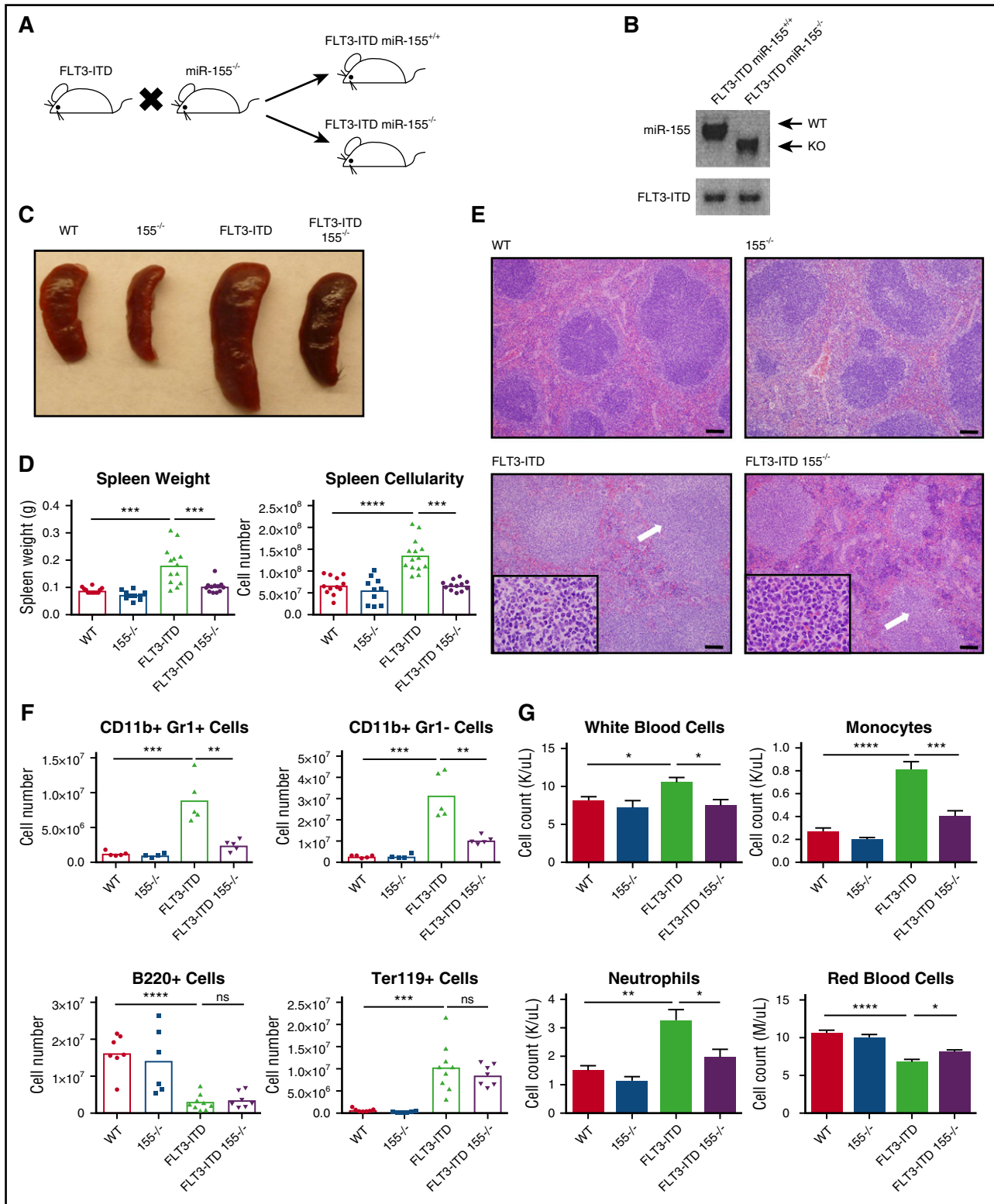
Figure 1. miR-155 promotes FLT3-ITD–mediated myeloid expansion in the spleen and blood. (A) Breeding strategy to create FLT3-ITD 155$^{-/-}$ mice. (B) PCR confirming the presence of FLT3-ITD and loss of miR-155. (C) Representative spleens for the different mouse groups. (D) Spleen size quantified by both weight and overall cellularity. (E) Hematoxylin and eosin staining of spleens from different mouse groups. Representative images are shown. White arrows denote areas of myeloproliferation. Full-sized images, original magnification ×100; inset, original magnification ×1000. Scale bar, 100 μm. (F) Total numbers of CD11b$^+$ Gr1$^+$ cells, CD11b$^+$ Gr1$^-$ cells, B220$^+$ cells, and Ter119$^+$ cells in the spleen determined by flow cytometry. (G) Complete blood counts for various blood cells in different mouse groups. Data are representative of at least 3 independent experiments. Each point represents a sample from 1 mouse. Data represented as mean ± SEM. *$P \leq$ .05; **$P \leq$ .01; ***$P \leq$ .001; ****$P \leq$ .0001; ns, $P >$ .05. KO, knockout.
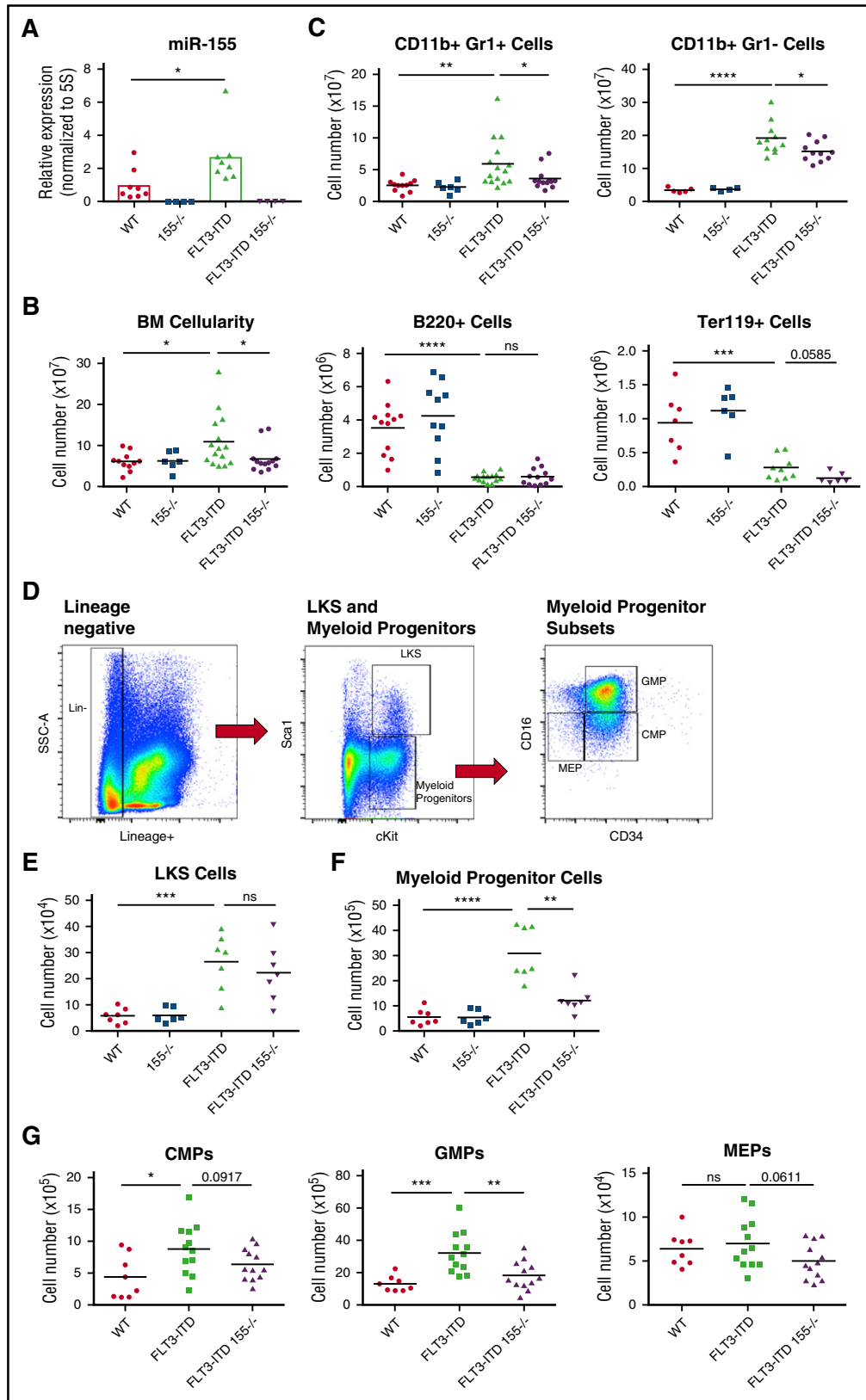
Figure 2. Expression of miR-155 in FLT3-ITD BM promotes expansion of myeloid progenitors. (A) Expression level of miR-155 in WT, 155[−/−], FLT3-ITD, and FLT3-ITD 155[−/−] mice in total BM determined by qRT-PCR. Expression normalized to 5S ribosomal RNA. (B) Total BM cellularity in different mouse groups. (C) Total numbers of CD11b^{+} Gr1^{+} cells, CD11b^{+} Gr1^{−} cells, B220^{+} cells, and Ter119^{+} cells in the BM of different mouse groups determined by flow cytometry. (D) Gating strategy for flow cytometric analysis of LKS and myeloid progenitor (Lin[−], c-Kit[+], Sca1^{−}) populations. (E) Total number of LKS cells in BM determined by flow cytometry. (F) Total number of myeloid progenitor cells (Lin[−], c-Kit[+], Sca1^{−}) in BM determined by flow cytometry. (G) Total common myeloid progenitor (CMP) (left), granulocyte-monocyte progenitor (middle), and megakaryocyte-erythrocyte progenitor (right) cells in BM determined by flow cytometry. Data are representative of at least 3 independent experiments. Each point represents a sample from 1 mouse. *$P \leq .05$; **$P \leq .01$; ***$P \leq .001$; ****$P \leq .0001$; ns, $P > .05$.
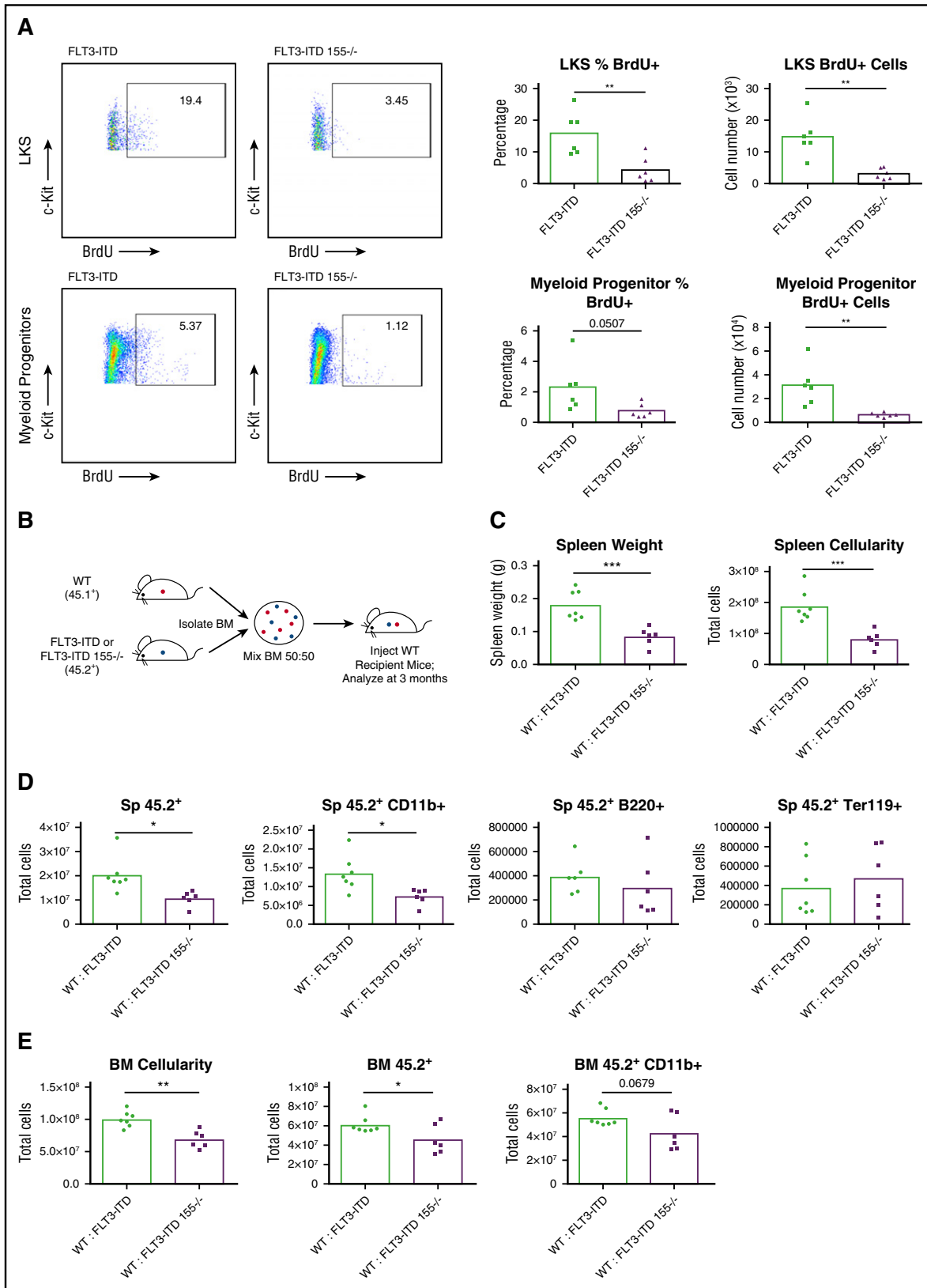
Figure 3. miR-155 promotes proliferation of the LKS and myeloid progenitor compartments and functions in a cell-intrinsic manner during FLT3-ITD–driven MPD. (A) Total BrdU[+] staining of LKS and myeloid progenitor cells (Lin[−], c-Kit[+], Sca1^{−}) in BM. Representative flow cytometric plots and percentages are shown. (B) Experimental strategy for producing WT:FLT3-ITD and WT:FLT3-ITD 155[−/−] BM chimeric mice. (C-D) Spleen analysis of WT:FLT3-ITD and WT:FLT3-ITD 155[−/−] BM chimeric mice at 3 months posttransplant. Total numbers of various cell populations determined by flow cytometry. (E) Analysis of BM from WT:FLT3-ITD and WT:FLT3-ITD 155[−/−] BM chimeric mice at 3 months posttransplant. Total numbers of various cell populations determined by flow cytometry. Data are representative of at least 2 independent experiments. Each point represents a sample from 1 mouse. *$P \leq .05$; **$P \leq .01$; ***$P \leq .001$.
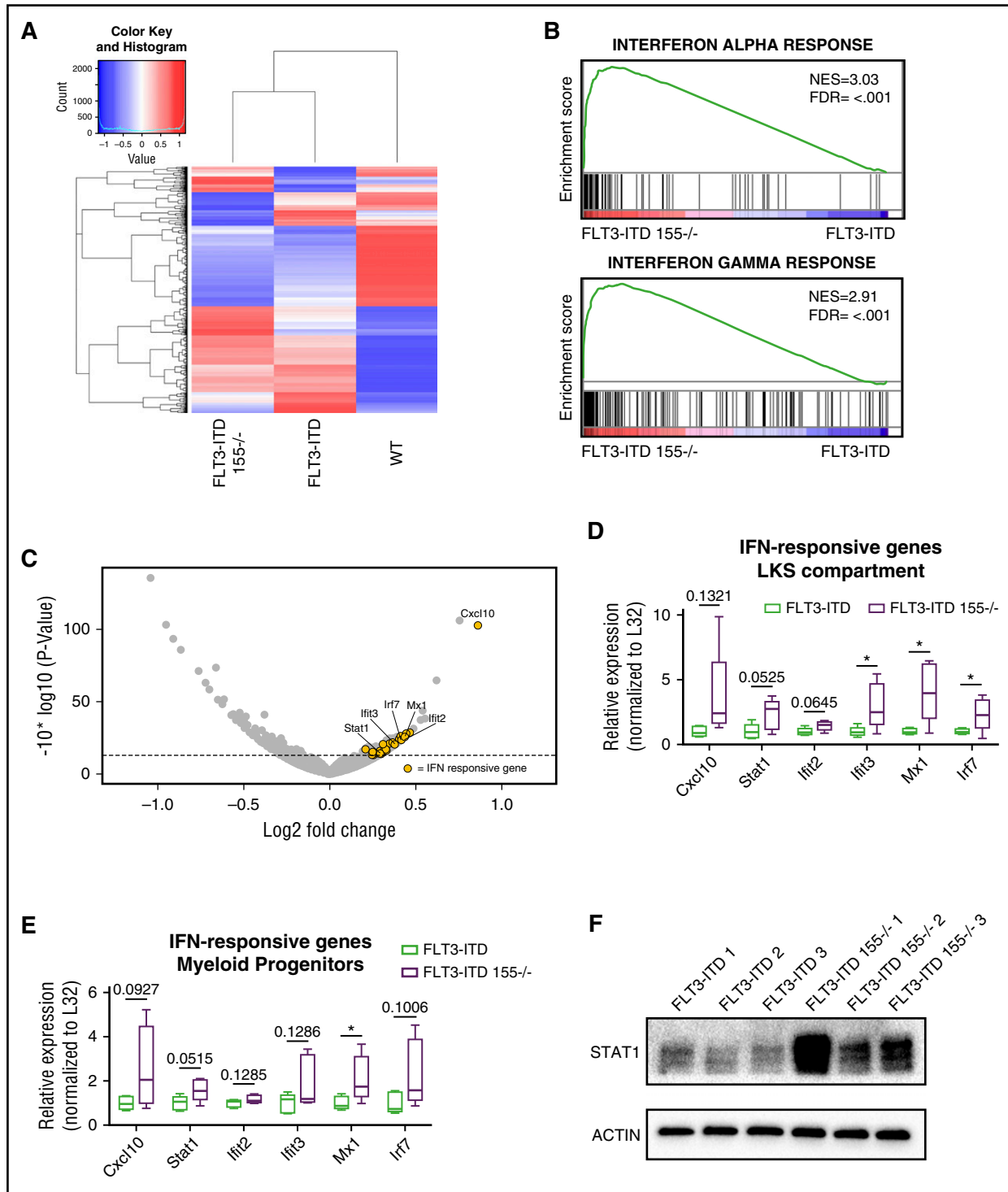
Figure 4. IFN signaling is increased in LKS and myeloid progenitor compartments of FLT3-ITD mice in the absence of miR-155. (A) Heat map showing gene expression differences in protein-coding genes identified by RNA sequencing of the LKS compartment of WT, FLT3-ITD, and FLT3-ITD 155$^{-/-}$ mice. (B) GSEA of LKS compartment RNA sequencing data identifies the IFN-α response and IFN-γ response as hallmark differences between FLT3-ITD and FLT3-ITD 155$^{-/-}$ mice. (C) Volcano plot showing LKS compartment gene expression changes in FLT3-ITD 155$^{-/-}$ vs FLT3-ITD mice. Dashed line represents a P value = .05. Yellow dots indicate IFN-α/γ–responsive genes as annotated by GSEA. (D-E) qRT-PCR analysis of representative IFN-responsive genes in the LKS or myeloid progenitor compartment of FLT3-ITD or FLT3-ITD 155$^{-/-}$ mice (n = 5 for each group). Expression normalized to L32, with the FLT3-ITD average set to a relative expression value of 1. (F) Western blot of STAT1 in LK-sorted BM of FLT3-ITD or FLT3-ITD 155$^{-/-}$ mice; replicates represent individual mice. ACTIN serves as the loading control. *$P \leq$ .05 FDR, false discovery rate; NES, normalized enrichment score.

counterparts. Flow cytometry on the spleen revealed a reduced total number of CD11b$^+$ Gr1$^-$ cells, primarily consisting of monocytes and dendritic cells, as well as a decrease in the neutrophilic CD11b$^+$ Gr1$^+$ population in the absence of miR-155 (Figure 1F; supplemental Figure 1A), indicating reduced splenic infiltration of mature myeloid cells.

In the peripheral blood, we observed a noticeable increase in white blood cells in the FLT3-ITD mice compared with WT mice, which is consistent with previous reports,[7] and this increase was significantly reduced in the FLT3-ITD 155$^{-/-}$ group (Figure 1G; supplemental Figure 1B). The decrease in leukocytosis in FLT3-ITD 155$^{-/-}$
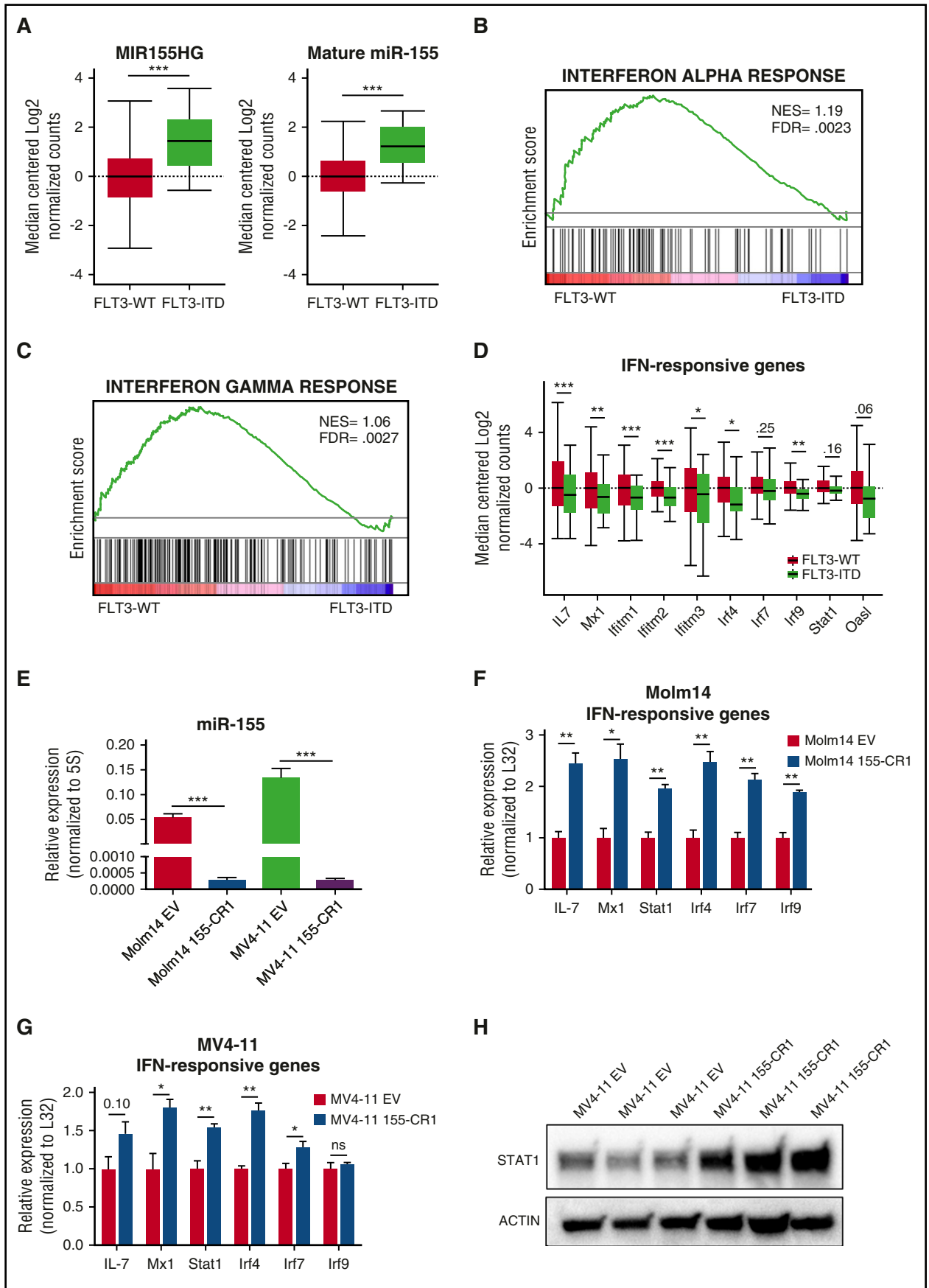
Figure 5.

compared with FLT3-ITD mice was attributed to decreased monocytosis and neutrophilia (Figure 1G). Although both FLT3-ITD and FLT3-ITD 155$^{-/-}$ mice were anemic, this phenotype was less severe when miR-155 was lacking. These findings demonstrate that deletion of miR-155 abrogates several aspects of the myeloproliferative phenotype observed in the spleen and blood of FLT3-ITD mice.

miR-155 drives myeloid cell production in the BM of FLT3-ITD mice by increasing granulocyte-monocyte progenitors

To determine the source of miR-155–dependent myeloproliferation in FLT3-ITD mice, we next analyzed the BM. FLT3-ITD BM cells displayed increased expression of miR-155 compared with BM from WT mice (Figure 2A), which is consistent with the clinical observation of elevated miR-155 levels in FLT3-ITD^{+} patient samples.[10,11] We also observed decreased BM cellularity in FLT3-ITD 155$^{-/-}$ compared with FLT3-ITD mice (Figure 2B). Flow cytometry revealed that this decrease in BM cellularity of FLT3-ITD 155$^{-/-}$ mice could largely be attributed to reduced CD11b^{+} Gr1^{+}, and CD11b^{+} Gr1^{-} cells (Figure 2C). In contrast, we did not observe a difference in the suppression of B220^{+} cells by FLT3-ITD when miR-155 was lacking. However, we did observe a slight decrease in Ter119^{+} cells in the BM of FLT3-ITD 155$^{-/-}$ mice compared with FLT3-ITD mice, suggesting that miR-155 may play some role in supporting erythroid development in the context of FLT3-ITD.

Next, we examined the impact of miR-155 on the HSPC population during FLT3-ITD–mediated disease. Total BM was isolated from the femurs and tibias of FLT3-ITD and FLT3-ITD 155$^{-/-}$ mice, and the depicted flow cytometry gating strategy was used to assess distinct HSPC populations (Figure 2D). There was no difference in the total number of LKS cells (Figure 2E), a compartment consisting of the earliest stem and progenitor cell populations.[25] However, there was a significant decrease in myeloid progenitor cells (Lin^{-}, c-Kit^{+}, Sca1^{-}) in FLT3-ITD 155$^{-/-}$ compared with FLT3-ITD mice (Figure 2F). This finding indicates that miR-155 is necessary for maintaining a robust myeloid progenitor pool in this disease context. On further analysis of myeloid progenitor subsets, we found that miR-155 is required for the increase in granulocyte-monocyte progenitor cells mediated by FLT3-ITD (Figure 2G; supplemental Figure 1C). We also observed a subtle decrease in megakaryocyte-erythrocyte progenitor cells in FLT3-ITD 155$^{-/-}$ mice, again suggesting that miR-155 may also be supporting erythroid development to some degree in FLT3-ITD animals. Altogether, these findings reveal a role for miR-155 in the myeloid progenitor compartment of the BM, where miR-155 is required for proper myeloid expansion in response to FLT3-ITD signaling.

miR-155 promotes the proliferation of the LKS and myeloid progenitor compartments in FLT3-ITD mice

After finding that miR-155 is critical for the myeloid-specific expansion seen in FLT3-ITD BM, we next sought to determine how miR-155 regulates myeloid cell numbers in the BM by assessing proliferation

and cell survival. Using a BrdU incorporation assay, we found that miR-155 promotes proliferation of both the LKS and myeloid progenitor cell populations (Figure 3A). However, on analyzing Annexin V levels, we did not see a miR-155–dependent difference in LKS and myeloid progenitor cells undergoing apoptosis when comparing FLT3-ITD and FLT3-ITD 155$^{-/-}$ mice (supplemental Figure 2A), suggesting that miR-155 plays a more specific role in promoting proliferation of these cells in this premalignant context. These data indicate that miR-155 enhances FLT3-ITD–mediated MPD by increasing the proliferation of LKS and myeloid progenitor cells in the hematopoietic compartment.

A hematopoietic cell–intrinsic role for miR-155 during FLT3-ITD–mediated MPD

To determine if miR-155 functions in a cell-intrinsic manner to promote FLT3-ITD–mediated MPD, we generated mice with BM chimeras and assessed different disease parameters. Irradiated WT recipient mice were reconstituted with equal cell numbers of WT (45.1^{+}) BM and FLT3-ITD or FLT3-ITD 155$^{-/-}$ (45.2^{+}) BM and were analyzed at 3 months postreconstitution (Figure 3B). Markedly increased splenomegaly was observed in the WT:FLT3-ITD compared with WT:FLT3-ITD 155$^{-/-}$ mice (Figure 3C), a finding that correlated with the expansion of FLT3-ITD 45.2^{+} cells, namely 45.2^{+} CD11b^{+} myeloid cells, compared with FLT3-ITD 155$^{-/-}$ cells (Figure 3D). WT:FLT3-ITD animals also had increased BM cellularity compared with their WT:FLT3-ITD 155$^{-/-}$ counterparts, with an increased number of 45.2^{+} white blood cells that included 45.2^{+} CD11b^{+} myeloid cells (Figure 3E). Both the FLT3-ITD and FLT3-ITD 155$^{-/-}$ 45.2^{+} cells dominated the BM engraftment at 3 months postreconstitution (supplemental Figure 2B-C), and we did not observe significant differences in the small number of remaining WT 45.1^{+} BM cells between groups (supplemental Figure 2D). These findings indicate that miR-155 plays a hematopoietic cell–intrinsic role as it promotes the expansion of FLT3-ITD^{+} myeloid cells.

miR-155 inhibits endogenous IFN signaling in LKS cells and myeloid progenitors from FLT3-ITD mice

To decipher the mechanism by which miR-155 promotes proliferation of the LKS and myeloid progenitor pool, we performed RNA sequencing of sorted cells from the LKS compartment of WT, FLT3-ITD, and FLT3-ITD 155$^{-/-}$ mice. Interestingly, although the gene expression profiles of FLT3-ITD and FLT3-ITD 155$^{-/-}$ samples clustered away from the WT group, they also exhibited distinct gene expression patterns (Figure 4A). We then performed Ingenuity Pathway Analysis and GSEA to determine which pathways were impacted according to the observed gene expression differences. Overwhelmingly, the results pointed to the IFN response as being highly upregulated in the absence of miR-155 (Figure 4B; supplemental Figure 3A-B). IFN-α– and IFN-γ–responsive genes, as determined by GSEA, made up a large proportion of genes that were significantly elevated in FLT3-ITD cells lacking miR-155

Figure 5. The TCGA data set of human AML samples and miR-155 mutant AML cell lines identify an inverse correlation between miR-155 levels and the IFN response in FLT3-ITD^{+} AML. (A) Box plot showing MIR155HG and mature miR-155 expression levels in FLT3-WT and FLT3-ITD AML samples from the TCGA data set. (B-C) GSEA of the TCGA data set identifies the IFN-α response and IFN-γ response as hallmark differences between FLT3-ITD AML and FLT3-WT AML. (D) Expression level of representative IFN-responsive genes from the TCGA data set in FLT3-WT and FLT3-ITD AML. (E) Relative expression of miR-155 in Molm14 and MV4-11 cells infected with EV or 155-CR1 vectors determined by qRT-PCR. Expression normalized to 5S. n = 3 biological replicates for each condition. (F-G) qRT-PCR analysis of representative IFN-responsive genes in Molm14 (F) or MV4-11 (G) cells infected with either EV or 155-CR1 vectors. Expression normalized to L32, with the EV-infected cell average set to a relative expression value of 1. n = 3 biological replicates for each condition. (H) Western blot of STAT1 in MV4-11 cells infected with either EV or 155-CR1 constructs. Replicates represent cells grown in independent wells for 72 hours. ACTIN serves as the loading control. LentiCRISPR data represent at least 2 independent experiments. Data represented as mean ± SEM. *$P \leq$ .05; **$P \leq$ .01; ***$P \leq$ .001; ns, $P >$ .05. FDR, false discovery rate; NES, normalized enrichment score.
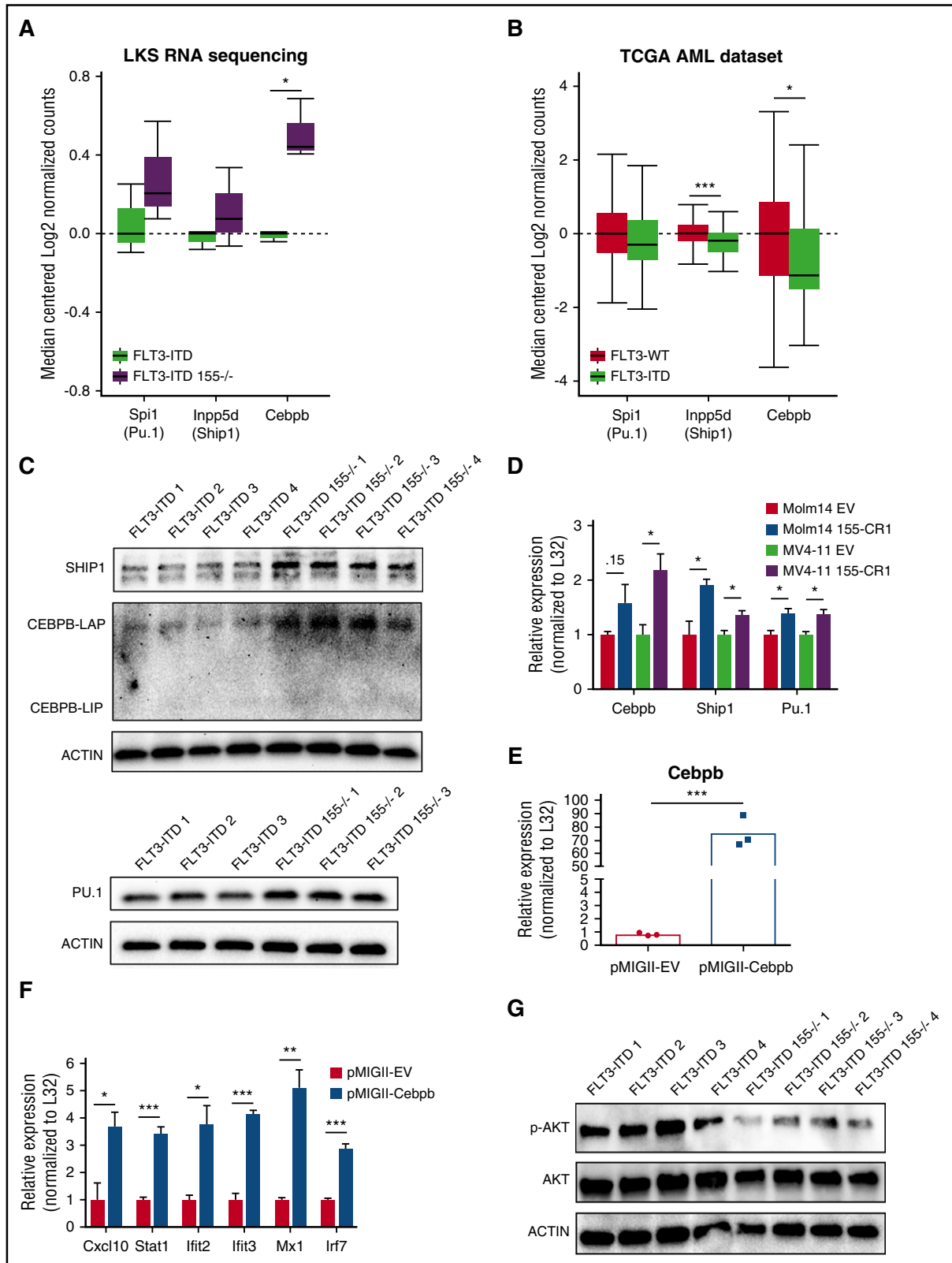
Figure 6. miR-155 represses multiple targets in mouse FLT3-ITD LK and human FLT3-ITD⁺ AML cells, including the IFN gene regulator Cebpb. (A) Expression level of miR-155 targets in the LKS compartment of FLT3-ITD or FLT3-ITD 155$^{-/-}$ mice by RNA sequencing. (B) Expression level of miR-155 targets in the TCGA human AML data set. (C) Western blot of SHIP1, PU.1, and CEBPB in LK-sorted BM of FLT3-ITD or FLT3-ITD 155$^{-/-}$ mice; replicates represent individual mice. (D) qRT-PCR analysis of miR-155 targets Cebpb, Ship1, and Pu.1 in Molm14 and MV4-11 cells infected with either EV or 155-CR1 constructs. Expression normalized to L32, with the EV-infected cell average set to a relative expression value of 1. n = 3 biological replicates for each condition. (E-F) qRT-PCR analysis of FLT3-ITD LK cells infected with either the pMIGII-EV or pMIGII-Cebpb vector. Expression normalized to L32 with pMIGII-EV–infected cell average set to a relative expression value of 1. n = 3 biological replicates for each condition. (G) Western blot of phospho-AKT (p-AKT) and total AKT of LK cells from FLT3-ITD and FLT3-ITD 155$^{-/-}$ mice; replicates represent individual mice. Data represented as mean ± SEM. *$P \leq .05$; **$P \leq .01$; ***$P \leq .001$.
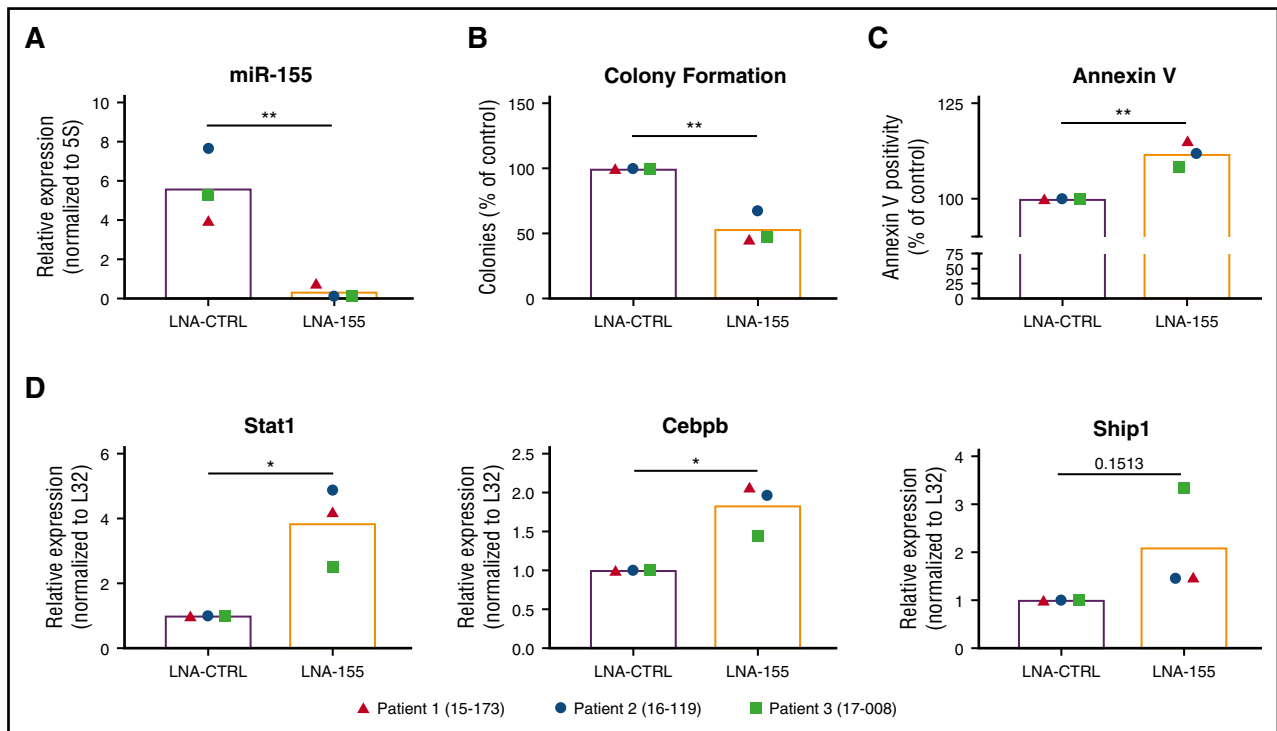
Figure 7. miR-155 promotes colony-forming potential and represses Cebpb and Stat1 expression in primary FLT3-ITD⁺ AML cells. (A) miR-155 expression in primary FLT3-ITD⁺ AML samples treated with a CTRL LNA or miR-155 LNA determined by qRT-PCR. Expression normalized to 5S ribosomal RNA. (B) Colony-forming potential of primary FLT3-ITD⁺ AML samples grown in methylcellulose agar supplemented with 100 nM CTRL LNA or miR-155 LNA. (C) Annexin V staining of primary FLT3-ITD⁺ AML samples treated with CTRL LNA or miR-155 LNA for 3 days in liquid culture. (D) qRT-PCR analysis of primary FLT3-ITD⁺ AML samples treated with CTRL LNA or miR-155 LNA. Expression normalized to L32, with LNA-CTRL treated cell average set to a relative expression of 1. Each point represents an individual patient sample. $*P \leq .05$; $**P \leq .01$.

(Figure 4C; supplemental Figure 3C-D). Interestingly, although we found that the IFN response was moderately elevated in FLT3-ITD compared with WT LKS cells (supplemental Figure 4A), it was further increased in the FLT3-ITD $155^{-/-}$ group, suggesting that the absence of miR-155 impairs the ability of FLT3-ITD to suppress the antiproliferative effect of BM regulatory cytokines. We further validated these RNA sequencing data using qRT-PCR to assay the expression levels of IFN-responsive genes in the LKS (Figure 4D) and myeloid progenitor compartments (Figure 4E), where we found the same overall trend in increased expression of IFN-responsive genes in the absence of miR-155, but only in the context of FLT3-ITD (supplemental Figure 4B-C). Lastly, we evaluated protein levels of STAT1, a master regulator of IFN responses, by western blotting and observed a large increase in STAT1 expression in FLT3-ITD LK cells deficient in miR-155 (Figure 4F). Altogether, these data support a model whereby miR-155 promotes proliferation of the LKS and myeloid progenitor pool in FLT3-ITD–mediated neoplasms by reducing the antiproliferative effects of IFN signaling in these cells.

Analysis of the TCGA human AML data set identifies increased miR-155 and decreased IFN signaling in FLT3-ITD⁺ AML

To extend our findings from an animal model of FLT3-ITD–mediated disease into the clinical arena, we next analyzed sequencing results from human AML samples deposited in TCGA.[26] We sorted these 173 samples according to FLT3 status, placing patients with duplications in the FLT3 juxtamembrane domain in the FLT3-ITD group and patients without mutations in FLT3 in the FLT3-WT group. We found that MIR155HG, the miR-155 host gene, and mature miR-155

were significantly increased in FLT3-ITD⁺ AML samples compared with FLT3-WT AML samples (Figure 5A), which is consistent with previous reports.[10-13] Next, we further analyzed these gene expression data from the categorized FLT3-WT and FLT3-ITD groups using GSEA and demonstrated that both the IFN-α and IFN-γ responses were significantly downregulated in FLT3-ITD⁺ AML compared with FLT3-WT AML (Figure 5B-C), revealing an inverse correlation with miR-155 levels in FLT3-ITD⁺ AML. This reduction can also be appreciated by examining the expression of representative IFN-responsive genes between the 2 groups (Figure 5D).

To further examine the connection between miR-155 and the IFN response, we deleted miR-155 in FLT3-ITD⁺ human AML cell lines (MV4-11 and Molm14). Cells were transduced by using a previously developed miR-155 targeting lentiviral CRISPR/Cas9 construct (155-CR1),[19] and we subsequently observed significant miR-155 knockdown in both Molm14 and MV4-11 cell lines (Figure 5E). Reduced levels of miR-155 in Molm14 and MV4-11 cells resulted in significantly increased IFN signaling compared with cells infected with EV control (Figure 5F-G). In addition, we observed increased STAT1 protein levels in MV4-11 155-CR1 cells (Figure 5H). Together, these findings strongly correlate with data in our FLT3-ITD mouse model.

Multiple direct miR-155 targets are increased in FLT3-ITD⁺ myeloid cells in the absence of miR-155, including the IFN regulator Cebpb

To determine which of the direct targets of miR-155 are involved in its regulation of FLT3-ITD–mediated disease, we first analyzed the expression of established miR-155 targets in our LKS sequencing data

set. Ship1, Pu.1, and Cebpb have all previously been shown by us and others to be directly targeted by miR-155[17,27] and may play important miR-155–dependent roles in FLT3-ITD pathogenesis.[18,28,29] We found increased expression of these targets in FLT3-ITD 155[−/−] compared with FLT3-ITD mice, with a statistically significant increase in Cebpb (Figure 6A). In the human AML TCGA data set, we found that expression of Spi1 (Pu.1), Inpp5d (Ship1), and Cebpb was lower in FLT3-ITD[+] AML, with Ship1 and Cebpb reaching statistical significance (Figure 6B). Expression of these genes also inversely correlates with the higher expression of miR-155 (supplemental Figure 5), suggesting that they could be functional miR-155 targets in this disease setting. Next, we sorted LK cells from FLT3-ITD and FLT3-ITD 155[−/−] mice and evaluated protein levels of these miR-155 targets via western blot. Elevated expression of all 3 of these proteins was observed in FLT3-ITD 155[−/−] vs FLT3-ITD mice (Figure 6C), which is consistent with each of these being directly repressed by miR-155 in vivo. We also observed higher transcript levels of these targets in our 155-CR1–infected human FLT3-ITD[+] cell lines (Figure 6D).

The miR-155 target Cebpb has previously been implicated in the regulation of IFN signaling.[30-32] To determine if elevated Cebpb levels could increase the IFN response, we overexpressed Cebpb in sorted LK cells (Figure 6E) and observed increased expression of IFN-responsive genes (Figure 6F). This was also true in Cebpb-overexpressing RAW264.7 cells, a murine myeloid cell line, treated with recombinant type I and type II IFN (supplemental Figure 6). This finding demonstrates that Cebpb is sufficient to induce the IFN response in myeloid cells and supports a model whereby miR-155 repression of Cebpb is involved in its ability to repress the IFN response in myeloid cells.

We also examined the downstream effect of miR-155's repression of Ship1, a known inhibitor of AKT activation.[33] Consistent with elevated Ship1 levels in FLT3-ITD 155[−/−] cells, we observed decreased AKT phosphorylation in the LK cells of FLT3-ITD 155[−/−] mice compared with FLT3-ITD mice (Figure 6G). Taken together, this finding indicates that miR-155 works through a multitarget mechanism that enables regulation of multiple relevant signaling pathways and responses that define FLT3-ITD myeloid cell biology.

Inhibition of miR-155 in primary FLT3-ITD[+] AML samples leads to decreased colony formation and increased Stat1 expression

To assess the functional role of miR-155–mediated regulation of the IFN response in primary FLT3-ITD[+] AML, we treated primary AML samples (n = 3, supplemental Table 1) with an LNA antisense oligonucleotide targeting miR-155 (LNA-155) or a scrambled control LNA oligonucleotide (LNA-CTRL) and assessed these cells for changes in the expression of Stat1, as well as colony formation in methylcellulose medium and Annexin V positivity. qRT-PCR confirmed miR-155 inhibition by LNA-155 at 100 nM (Figure 7A), and this correlated with a reduction of colony formation (Figure 7B) and an increase in apoptosis (Figure 7C). Consistent with data in our mouse model, miR-155 inhibition in primary FLT3-ITD[+] AML samples correlated with increased expression of Stat1, Cebpb, and Ship1 (Figure 7D). These results provide further evidence that our findings in mice extend to primary human FLT3-ITD^{+} AML cells.

Discussion

miRNA expression is highly dysregulated in FLT3-ITD[+] AML, a subtype of AML that confers a poor prognosis. Microarray and qRT-PCR–based methods have shown that miR-155 is among the most highly overexpressed miRNAs in FLT3-ITD[+] AML.[10-16] We further substantiated these findings by analyzing the TCGA human AML data set, which contains sequencing data from 173 patients representing all major subtypes of AML. Our retrospective analysis confirmed that miR-155 was the most significantly upregulated miRNA in FLT3-ITD[+] AML compared with FLT3-WT AML.

From a functional perspective, miR-155 has been shown by our group and others to be important for the growth of FLT3-ITD^{+} cells in vitro.[18,19] We recently identified miR-155 as a top growth-promoting miRNA in a FLT3-ITD[+] leukemic cell line via a genome-wide CRISPR/Cas9 screen.[19] Importantly, both FLT3-ITD and miR-155 overexpression are each sufficient to cause MPDs in mice.[7-9,17] However, the impact of endogenous miR-155 on FLT3-ITD–mediated disease in vivo had not been previously explored. In the current study, we crossed FLT3-ITD and miR-155^{−/−} mice to determine if these 2 molecules collaborate to induce MPD. Indeed, we found that miR-155 is critical for several aspects of disease development in FLT3-ITD mice, including myeloid expansion in the BM, spleen, and peripheral blood. Further analysis of the hematopoietic compartment revealed that miR-155 promotes disease in FLT3-ITD mice by increasing proliferation of the LKS and myeloid progenitor compartments.

Through RNA sequencing of the LKS compartment, we identified the IFN response as being substantially increased in FLT3-ITD 155[−/−] compared with FLT3-ITD mice. We also demonstrated that human FLT3-ITD[+] AML samples had increased miR-155 and a decreased IFN gene expression signature when compared with FLT3-WT AML, which is consistent with our mouse data. It is well established that IFN signaling has growth-inhibitory effects on the hematopoietic compartment,[20-23] and inhibition of IFN signaling was recently discovered as a novel mechanism by which FLT3-ITD^{+} cells can avoid the antiproliferative effects of IFN-α and IFN-γ.[24] Our results indicate that miR-155 is clearly involved in this mechanism that subverts the antiproliferative effects of IFN in this setting. Our findings are also in line with a recent study demonstrating that miR-155 promotes proliferation of CD8^{+} T cells through inhibition of IFN signaling,[34] indicating that this mechanism is used by multiple cell types in vivo. Taken together, this work provides novel insights into the role of miR-155 in FLT3-ITD–mediated disease, where it helps HSPCs to escape the growth-inhibitory effects that are typically conferred by regulatory BM cytokines.

A number of studies have found that miR-155 can repress the expression of selected relevant targets, such as Ship1, Cebpb, and Pu.1, within FLT3-ITD[+] AML cell lines.[18,28,29] Furthermore, we found that both Ship1 and Cebpb were decreased at the RNA level in FLT3-ITD vs FLT3-WT AML patient samples. To better understand our in vivo phenotype, we examined the regulation of these targets by miR-155 in sorted LKS and myeloid progenitors and found that these targets are indeed derepressed in early stem cell compartments genetically deficient for miR-155. Of note, Pu.1 and Cebpb are well-known myeloid commitment genes,[35] and reduction in either Ship1 or Pu.1 levels can give rise to myeloproliferation,[27,36] which further supports the functional relevance of their regulation by miR-155 in this context. In the case of Cebpb, it has been previously shown to promote the IFN response,[30-32] providing a connection between miR-155 and the repression of IFN-responsive genes. Indeed, we found that Cebpb could enhance the IFN response in murine myeloid cells, including LK cells. We also showed that AKT was less activated in the LK cells of FLT3-ITD 155[−/−] mice, likely due to increased levels of the miR-155 target and known AKT inhibitor, Ship1. Taken together, our data indicate that miR-155 acts on multiple targets, suggesting a complex mechanism of action that could involve both IFN signaling–dependent and –independent mechanisms. Sorting out the individual contributions of these targets to

the IFN response and/or additional mechanisms at play in this context will be a fascinating future area of study.

Our current results, coupled with other clinical observations that miR-155 upregulation correlates with the FLT3-ITD[+] subtype of AML that confers a negative prognosis, provide a physiologically relevant context where miR-155 plays a deleterious role in the myeloid compartment in vivo. We also demonstrate a functional role for miR-155 in FLT3-ITD[+] AML, because inhibition of miR-155 reduced survival and increased apoptosis in primary FLT3-ITD[+] AML samples, and this correlated with increased expression of Stat1, Cebpb, and Ship1. Taken as a whole, the current study provides strong evidence that miR-155 promotes FLT3-ITD–mediated MPD, at least in part, through its regulation of IFN signaling in the early hematopoietic compartment and argues that therapeutic targeting of miR-155 in FLT3-ITD[+] AML may warrant serious consideration.

Authorship

Contribution: J.A.W. and R.M.O. designed the study; J.A.W., D.A.K., A.M.E., C.N.K., R.H., M.C.R., M.A., T.B.H., S.-H.L., and W.P.V. performed the experiments; T.L.M. performed the bioinformatics analysis; D.S.R. and R.R.M. performed the histopathology; J.A.W., D.A.K., J.L.R., and R.M.O. performed the data analysis; M.W.D. and A.B.P. provided patient samples; and J.A.W. and R.M.O. wrote the manuscript.

Conflict-of-interest disclosure: The authors declare no competing financial interests.

Correspondence: Ryan M. O'Connell, Department of Pathology, University of Utah, 15 North Medical Dr East, Salt Lake City, UT 84112; e-mail: ryan.oconnell@path.utah.edu.

References

1. Ferrara F, Schiffer CA. Acute myeloid leukaemia in adults. *Lancet*. 2013;381(9865): 484-495.

2. Small D, Levenstein M, Kim E, et al. STK-1, the human homolog of Flk-2/Flt-3, is selectively expressed in CD34+ human bone marrow cells and is involved in the proliferation of early progenitor/stem cells. *Proc Natl Acad Sci USA*. 1994;91(2):459-463.

3. Levis M, Small D. FLT3: ITDoes matter in leukemia. *Leukemia*. 2003;17(9):1738-1752.

4. Greenblatt S, Li L, Slape C, et al. Knock-in of a FLT3/ITD mutation cooperates with a NUP98-HOXD13 fusion to generate acute myeloid leukemia in a mouse model. *Blood*. 2012; 119(12):2883-2894.

5. Schessl C, Rawat VP, Cusan M, et al. The AML1-ETO fusion gene and the FLT3 length mutation collaborate in inducing acute leukemia in mice. *J Clin Invest*. 2005;115(8):2159-2168.

6. Shih AH, Jiang Y, Meydan C, et al. Mutational cooperativity linked to combinatorial epigenetic gain of function in acute myeloid leukemia. *Cancer Cell*. 2015;27(4):502-515.

7. Lee BH, Tothova Z, Levine RL, et al. FLT3 mutations confer enhanced proliferation and survival properties to multipotent progenitors in a murine model of chronic myelomonocytic leukemia. *Cancer Cell*. 2007;12(4):367-380.

8. Kelly LM, Liu Q, Kutok JL, Williams IR, Boulton CL, Gilliland DG. FLT3 internal tandem duplication mutations associated with human acute myeloid leukemias induce myeloproliferative disease in a murine bone marrow transplant model. *Blood*. 2002;99(1):310-318.

9. Li L, Piloto O, Nguyen HB, et al. Knock-in of an internal tandem duplication mutation into murine FLT3 confers myeloproliferative disease in a mouse model. *Blood*. 2008;111(7): 3849-3858.

10. Garzon R, Garofalo M, Martelli MP, et al. Distinctive microRNA signature of acute myeloid leukemia bearing cytoplasmic mutated nucleophosmin. *Proc Natl Acad Sci USA*. 2008;105(10):3945-3950.

11. Whitman SP, Maharry K, Radmacher MD, et al. FLT3 internal tandem duplication associates with adverse outcome and gene- and microRNA-expression signatures in patients 60 years of age or older with primary cytogenetically normal acute myeloid leukemia: a Cancer and Leukemia Group B study. *Blood*. 2010;116(18):3622-3626.

12. Garzon R, Volinia S, Liu CG, et al. MicroRNA signatures associated with cytogenetics and prognosis in acute myeloid leukemia. *Blood*. 2008;111(6):3183-3189.

13. Ramamurthy R, Hughes M, Morris V, et al. miR-155 expression and correlation with clinical outcome in pediatric AML: a report from Children's Oncology Group. *Pediatr Blood Cancer*. 2016;63(12):2096-2103.

14. Jongen-Lavrencic M, Sun SM, Dijkstra MK, Valk PJ, Löwenberg B. MicroRNA expression profiling in relation to the genetic heterogeneity of acute myeloid leukemia. *Blood*. 2008;111(10): 5078-5085.

15. Cammarata G, Augugliaro L, Salemi D, et al. Differential expression of specific microRNA and their targets in acute myeloid leukemia. *Am J Hematol*. 2010;85(5):331-339.

16. Marcucci G, Maharry KS, Metzeler KH, et al. Clinical role of microRNAs in cytogenetically normal acute myeloid leukemia: miR-155 upregulation independently identifies high-risk patients. *J Clin Oncol*. 2013;31(17):2086-2093.

17. O'Connell RM, Rao DS, Chaudhuri AA, et al. Sustained expression of microRNA-155 in hematopoietic stem cells causes a myeloproliferative disorder. *J Exp Med*. 2008;205(3):585-594.

18. Gerloff D, Grundler R, Wurm AA, et al. NF-κB/STAT5/miR-155 network targets PU.1 in FLT3-ITD-driven acute myeloid leukemia. *Leukemia*. 2015;29(3):535-547.

19. Wallace J, Hu R, Mosbruger TL, et al. Genome-Wide CRISPR-Cas9 screen identifies microRNAs that regulate myeloid leukemia cell growth. *PLoS One*. 2016;11(4):e0153689.

20. Jiang LJ, Zhang NN, Ding F, et al. RA-inducible gene-I induction augments STAT1 activation to inhibit leukemia cell proliferation. *Proc Natl Acad Sci USA*. 2011;108(5):1897-1902.

21. Ersvaer E, Skavland J, Ulvestad E, Gjertsen BT, Bruserud Ø. Effects of interferon gamma on native human acute myelogenous leukaemia cells. *Cancer Immunol Immunother*. 2007;56(1):13-24.

22. Anguille S, Lion E, Willemen Y, Van Tendeloo VF, Berneman ZN, Smits EL. Interferon-α in acute myeloid leukemia: an old drug revisited. *Leukemia*. 2011;25(5):739-748.

23. Benjamin R, Khwaja A, Singh N, et al. Continuous delivery of human type I interferons (alpha/beta) has significant activity against acute myeloid leukemia cells in vitro and in a xenograft model. *Blood*. 2007;109(3):1244-1247.

24. Reddy PN, Sargin B, Choudhary C, et al; Study Alliance Leukemia (SAL). SOCS1 cooperates with FLT3-ITD in the development of myeloproliferative disease by promoting

the escape from external cytokine control. *Blood.* 2012;120(8):1691-1702.

25. Spangrude GJ, Heimfeld S, Weissman IL. Purification and characterization of mouse hematopoietic stem cells. *Science.* 1988; 241(4861):58-62.

26. Ley TJ, Miller C, Ding L, et al; Cancer Genome Atlas Research Network. Genomic and epigenomic landscapes of adult de novo acute myeloid leukemia. *N Engl J Med.* 2013;368(22):2059-2074.

27. O'Connell RM, Chaudhuri AA, Rao DS, Baltimore D. Inositol phosphatase SHIP1 is a primary target of miR-155. *Proc Natl Acad Sci USA.* 2009; 106(17):7113-7118.

28. Salemi D, Cammarata G, Agueli C, et al. miR-155 regulative network in FLT3 mutated acute myeloid leukemia. *Leuk Res.* 2015;39(8):883-896.

29. Khalife J, Radomska HS, Santhanam R, et al. Pharmacological targeting of miR-155 via the NEDD8-activating enzyme inhibitor MLN4924 (Pevonedistat) in FLT3-ITD acute myeloid leukemia. *Leukemia.* 2015;29(10): 1981-1992.

30. Li H, Gade P, Xiao W, Kalvakolanu DV. The interferon signaling network and transcription factor C/EBP-beta. *Cell Mol Immunol.* 2007;4(6): 407-418.

31. Roy SK, Wachira SJ, Weihua X, Hu J, Kalvakolanu DV. CCAAT/enhancer-binding protein-beta regulates interferon-induced transcription through a novel element. *J Biol Chem.* 2000;275(17):12626-12632.

32. Xiao W, Wang L, Yang X, et al. CCAAT/enhancer-binding protein beta mediates interferon-gamma-induced p48 (ISGF3-gamma) gene transcription

in human monocytic cells. *J Biol Chem.* 2001; 276(26):23275-23281.

33. Liu Q, Sasaki T, Kozieradzki I, et al. SHIP is a negative regulator of growth factor receptor-mediated PKB/Akt activation and myeloid cell survival. *Genes Dev.* 1999;13(7):786-791.

34. Gracias DT, Stelekati E, Hope JL, et al. The microRNA miR-155 controls CD8(+) T cell responses by regulating interferon signaling. *Nat Immunol.* 2013;14(6):593-602.

35. Feng R, Desbordes SC, Xie H, et al. PU.1 and C/EBPalpha/beta convert fibroblasts into macrophage-like cells. *Proc Natl Acad Sci USA.* 2008;105(16):6057-6062.

36. Rosenbauer F, Wagner K, Kutok JL, et al. Acute myeloid leukemia induced by graded reduction of a lineage-specific transcription factor, PU.1. *Nat Genet.* 2004;36(6):624-630.